Supporting information

Synthesis and Atomic Characterization of a Ti_2O_3 Nanosheet

Megumi Ohwada,[*, †] *Koji Kimoto,*[*, †] *Kazutomo Suenaga,*[‡] *Yuta Sato,*[‡] *Yasuo Ebina,*[§] *Takayoshi Sasaki*[§]

[†, §] National Institute for Materials Science, Tsukuba, Ibaraki, Japan,

[‡]National Institute for Advanced Industrial Science and Technology, Tsukuba, Ibaraki, Japan

*To whom correspondence should be addressed. E-mail: ohwada.megumi@nims.go.jp (M.O.); kimoto.koji@nims.go.jp (K.K.).

1. Quantitative analysis of electron diffraction patterns

To confirm the crystal structure of a titania nanosheet and its reduced form, electron diffraction patterns were quantitatively analyzed. First, we compare the experimental result of the original TiO_2 titania nanosheet with a simulation result (Table S1). The experimental diffraction intensities were evaluated from the diffraction pattern (Figure 1a in the main text) obtained using a charge coupled device camera. The diffraction intensities of the reported structure[1,2] of the titania nanosheet were calculated using a multislice program (HREM Research Inc., xHREM). Since the diffraction intensities (e.g., I_{002} and I_{202}) are substantially weak compared with the transmitted electron intensity I_{000}, we compared the relative diffraction intensities normalized by the major reflection intensity of I_{200}. As shown in Table S1, the experimental and simulation results show good agreement, indicating the methodological validity of the electron diffraction analysis.

Table S1. Relative diffraction intensities of TiO_2 titania nanosheet.
The experimental intensities were obtained from Figure 1a.

	Diffraction intensity ratio						
	I_{002}/I_{200}	I_{202}/I_{200}	I_{101}/I_{200}	I_{100}/I_{200}	I_{102}/I_{200}	I_{201}/I_{200}	I_{001}/I_{200}
Experiment (Fig. 1a)	0.63	0.39	-	-	-	-	-
Simulation (TiO_2)	0.61	0.34	0.02	0	0	0	0

Electron diffraction analysis of the reduced titania nanosheet is shown in Table S2. We compare the experimental (Figure 1b) and simulation results of several crystal structures. We firstly constructed a face-shared Ti_2O_3 model (Figure 3b). However, the simulation result of this model does not reproduce the experimental result, particularly for the extra spot intensity I_{100}, as shown by (I) in Table S2. The strong 100 spot and the absence of the 001 spot in the experimental data suggest the movement of Ti

atoms along the *a*-axis based on the kinematical diffraction theory. We then calculated the diffraction intensities of the Ti_2O_3 models with varying Ti displacement, as shown by (II)-(V) in Table S2, in which δx denotes the displacement of Ti atoms from the center of each octahedron (blue one in Figure 3). For instance, a displacement of 19 pm corresponds to 1/20 of the lattice constant *a* (0.38nm). It is found that an atomic displacement of 38 pm along the *a*-axis well reproduces the experimental result.

Table S2. Experimental and simulation results of diffraction intensities of reduced titania nanosheet. The experimental intensities were obtained from Figure 1b. In the calculations, Ti atoms in the distorted octahedra are shifted by (II) 19, (III) 38, (IV) 57 and (V) 76 pm along the *a*-axis.

	Diffraction intensity ratio						
	I_{002}/I_{200}	I_{202}/I_{200}	I_{101}/I_{200}	I_{100}/I_{200}	I_{102}/I_{200}	I_{201}/I_{200}	I_{001}/I_{200}
Experiment (Fig. 1b)	0.80	0.33	0.05	0.33	0.10	0.16	-
Simulation (Ti_2O_3) with varying Ti displacement, δx (pm)							
(I) δx = 0 (Fig. 3b)	0.61	0.34	0.09	0.04	0.01	0.01	0.03
(II) δx = 19	0.67	0.33	0.10	0.08	0.02	0.03	0.03
(III) δx = 38 (Fig. 3c)	0.88	0.33	0.16	0.28	0.05	0.09	0.04
(IV) δx = 57	1.40	0.33	0.29	0.90	0.14	0.24	0.07
(V) δx = 76	2.63	0.33	0.63	2.75	0.41	0.59	0.13

2. Elemental and chemical bonding analyses by EELS

Elemental and chemical bonding analyses were performed using an aberration-corrected TEM (JEOL Ltd.)[3] equipped with a cold field-emission gun and an electron energy-loss spectrometer (Gatan Inc., low-voltage GIF). EEL spectra were acquired by image coupling,[4] in which the diffraction patterns were observed on a fluorescent screen. Figure S1a shows the EEL spectra at different electron doses.

The spectra were acquired before (1), after (2) and (3) extra spots appeared in the diffraction pattern. The dependence of the atomic ratio on electron dose was calculated from the integrated intensity of the O-*K* edge and Ti-*L* edges. The atomic ratio O/Ti is found to be (1) 2.2, (2) 1.4 and (3) 1.0. It is clear that the electron irradiation induced the reduction of the specimen. Figure S1b shows enlarged Ti-*L* edges. The Ti L_3 and L_2 edges of the initial TiO_2 nanosheet show the crystal field splitting, as denoted by arrows. The Ti-*L* edges at high electron doses show a chemical shift to lower energy losses, which also corresponds to the reduction of the specimen.[5] In addition, the crystal field splitting disappears at high electron doses, suggesting the change in the symmetry of TiO_6 octahedra.

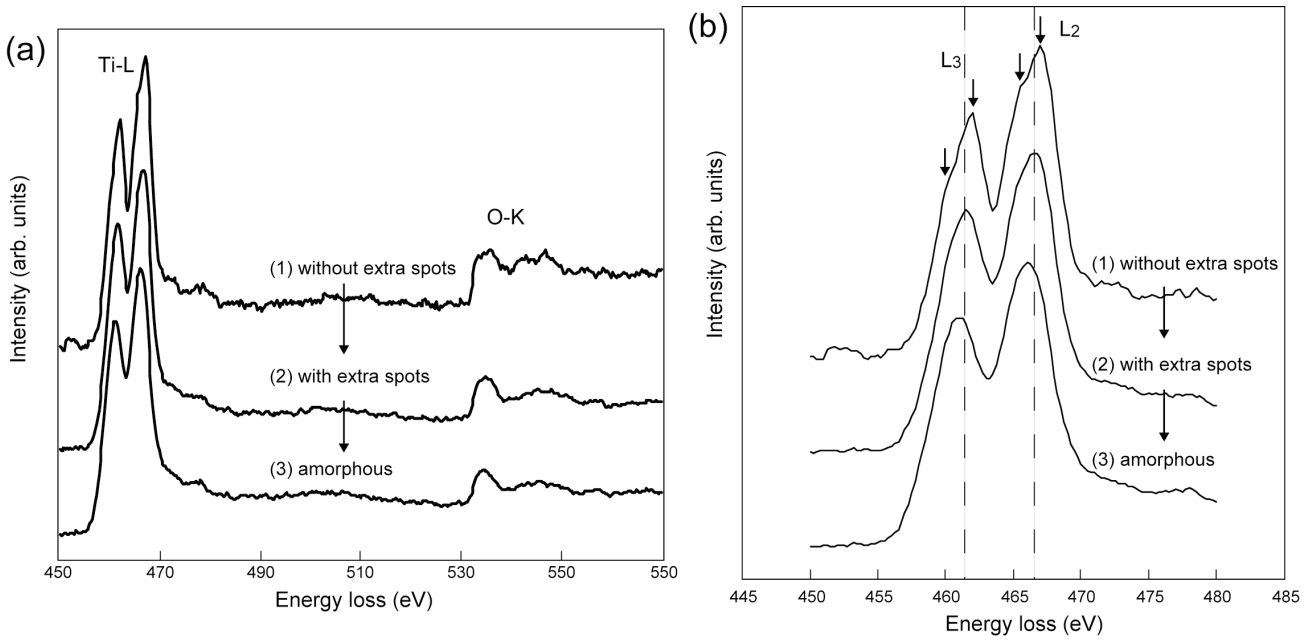

Figure S1. EELS analyses showing reduction of titania nanosheet by electron irradiation. (a) EEL spectra of Ti-*L* and O-*K* edges acquired at different electron doses. (b) Enlarged Ti-*L* edges: (1) TiO_2 nanosheet without extra spots in diffraction pattern, (2) Ti_2O_3 nanosheet with extra spots, and (3) damaged amorphous film.

3. Relatively low-magnification TEM image of Ti_2O_3 nanosheet

The lateral size of the delaminated TiO_2 nanosheet is on the micrometer order, and we observed sub-micrometer-order Ti_2O_3 nanosheets. Figure S2 shows an example of the Ti_2O_3 nanosheets. 0.38 nm fringes, which suggest the Ti_2O_3 structure, are observed in the entire area.

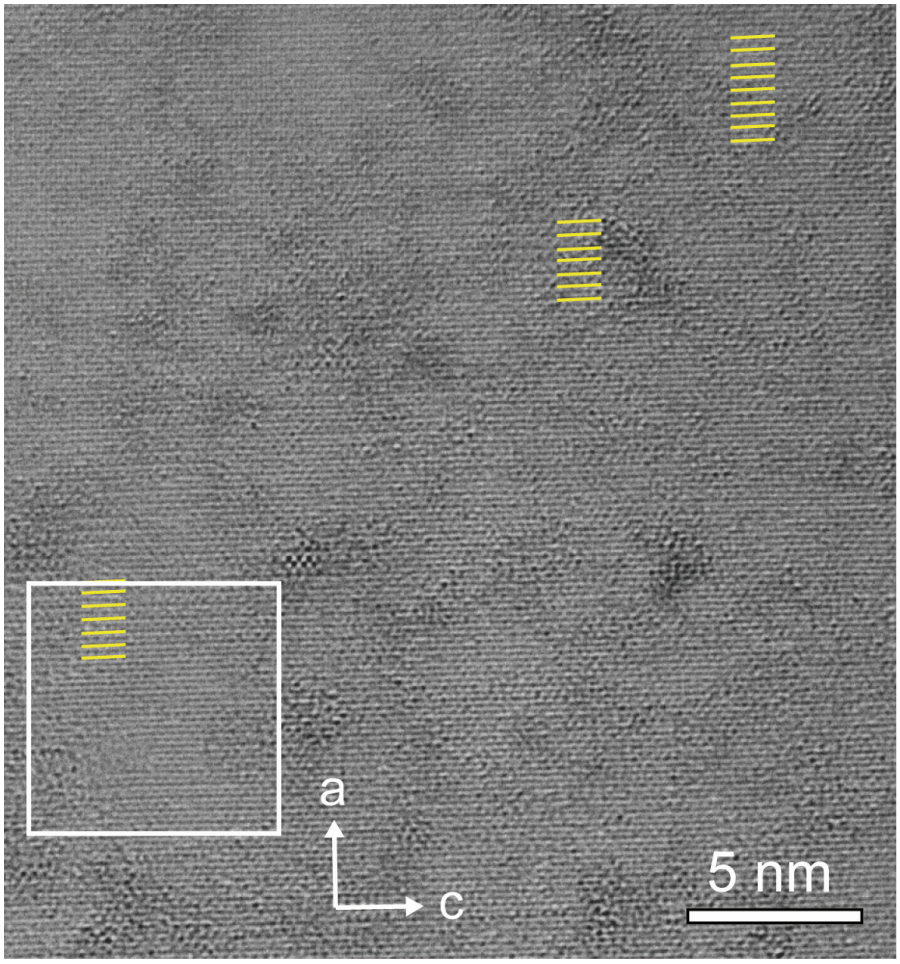

Figure S2. Example of TEM images of Ti_2O_3 nanosheet. The lines indicate 0.38nm fringes. The square in the lower left corresponds to the area of Figure 2a in the main text.

References

(1) Fukuda, K.; Nakai, I.; Oishi, C.; Nomura, M.; Harada, M.; Ebina, Y.; Sasaki, T. Nanoarchitecture of Semiconductor Titania Nanosheets Revealed by Polarization-Dependent Total Reflection Fluorescence X-ray Absorption Fine Structure. *J. Phys. Chem. B* **2004,** *108*, 13088-13092.

(2) Grey, I. E.; Li, C.; Madsen, I. C.; Watts, J. A. The Stability and Structure of $Cs_x[Ti_{2-x/4}\square_{x/4}]O_4$, $0.61<x<0.65$. *J. Solid State Chem.* **1987,** *66*, 7-19.

(3) Sasaki, T.; Sawada, H.; Hosokawa, F.; Kohno, Y.; Tomita, T.; Kaneyama, T.; Kondo, Y.; Kimoto, K.; Sato, Y.; Suenaga, K. Performance of Low-Voltage STEM/TEM with Delta Corrector and Cold Field Emission Gun. *J. Electron Microsc.* **2010,** *59*, S7-S13.

(4) Egerton, R. F. *Electron Energy-loss Spectroscopy in the Electron Microscope*. 2nd ed.; Elsevier: New York, 1996.

(5) Stoyanov, E.; Langenhorst, F.; Steinle-Neumann, G. The Effect of Valence State and Site Geometry on Ti $L_{3,2}$ and O *K* Electron Energy-Loss Spectra of Ti_xO_y phases. *Am. Mineral.* **2007,** *92*, 577-586.